PHYSICAL REVIEW B **81**, 155447 (2010)

Calculated cleavage behavior and surface states of LaOFeAs

Helmut Eschrig, Alexander Lankau, and Klaus Koepernik*
IFW Dresden, P.O. Box 270116, D-01171 Dresden, Germany
(Received 7 January 2010; revised manuscript received 10 March 2010; published 22 April 2010)

The layered structure of the iron-based superconductors gives rise to a more or less pronounced two dimensionality of their electronic structure, most pronounced in LaOFeAs. Consequences are distinct surface states to be expected to influence any surface sensitive experimental probe. In this work a detailed density-functional analysis of the cleavage behavior and the surface electronic structure of LaOFeAs is presented. The surface states are obtained to form two-dimensional bands with their own Fermi surfaces markedly different from the bulk electronic structure.

DOI: 10.1103/PhysRevB.81.155447 PACS number(s): 68.35.bd, 74.20.Pq, 74.25.Jb, 74.70.Xa

I. INTRODUCTION

About two years after the discovery of the high-T_c superconductor La(O,F)FeAs[1] its normal state electronic structure remains poorly understood. Although there is growing opinion that it is not a highly correlated case of Mott-Hubbard type,[2] its magnetic properties for instance are not at all well described by the local density approximations (LDA) of density-functional theory (DFT) or generalized gradient corrections (GGA) to it. In contrast to the cuprates where it was nearly immediately clear that the electronic structure of the cuprate plane is dominated by a $3d^9$ shell with a correlation localized hole in a single band, here a complex multiband case is obviously operative.[3] Like in the cuprates the electronic structure and most properties are highly anisotropic though to varying extent.[4]

Many experimental probes of the electronic structure, photoemission in particular, are surface sensitive. To assess these experiments it is crucial to know something on the surface structure and possible surface states of the material. So far, as a rule those experiments are interpreted in terms of the bulk electronic structure. Even if bulk properties show up in the experiment, the possible presence of surface states remains an important issue to be taken into account.

In this paper, the formation of surfaces in cleaving a single crystal and their properties are analyzed by means of DFT calculations for the most two-dimensional case, undoped LaOFeAs. A pronounced surface electronic structure is found for both forming surfaces, As and La terminated, which dramatically differs from the bulk electronic structure. All calculations are done within the nonmagnetic GGA model of LaOFeAs which fairly correctly describes the crystal structure of the material. The results presented here refer to samples, which are not magnetically ordered. Although the relevance of this model for electronic many-body behavior may be debated, the results on the surface relaxation and on the character of surface states must be considered relevant. The paramagnetism of local moments cannot be described in DFT. However, it will influence the low energy physics at most on a 100 meV scale.

The computational approach is described in the following section, while the results are presented and discussed in Sec. III. A short summary completes the paper.

II. COMPUTATIONAL APPROACH

All calculations were done by using the full-potential local-orbital (FPLO) code version FPLO9.00.[5] Relativistic effects were incorporated on a scalar relativistic level. The $\boldsymbol{k}$-mesh input parameters were set to 6,6,4 (number of $\boldsymbol{k}$ intervals along the a, b, and c axes of the Brillouin zone) for bulk calculations and to 6,6,2 for slab supercell calculations. Some calculations were repeated with parameters 12,12,4 and 12,12,2, respectively, with essentially no changes in the results. The density convergence parameter was always put to 10^{-6}.

Since the surface structures were relaxed before calculating the surface Kohn-Sham band structure, relaxed bulk reference structures had to be used for comparison. The obtained structure parameters together with experimental values are shown in Table I. Since as usually the GGA (Ref. 6) results are closer to experiment than the LDA (Ref. 7) results, the GGA functional was used in all further calculations. In this text tetragonal structures are considered only, therefore the low temperature experimental structure data from Ref. 8 were tetragonally averaged in Table I. As usual, z_O was put to zero and z_{Fe} to 1/2. We are interested in the (001) surfaces of bulk crystals, so the a lattice constant is kept fixed at the GGA bulk value $a=4.041$ Å in all what follows. In this text, the tetragonal axis of the structure is referred to as c axis and its direction as z direction.

The Kohn-Sham band structure of the GGA relaxed bulk crystal is shown in Fig. 1. The "fat bands" (online in red) on this figure indicate the O-2p and La-4f,5d,6s orbital character of the bands. The thickness of those fat bands is proportional to the sum of squares of coefficients for these basis states in the expansion of the Kohn-Sham wave function into the FPLO orbital basis. The Fermi level is put to zero in all presented band structures in this work. As is seen, the conduction states at Fermi level and in the occupied region of the conduction bands have very small wave function amplitudes in the LaO layers (cf. Fig. 2 for the layered structure). As has already been stated many times, they have predominantly Fe-3d character and decay exponentially into the LaO layers. Experimentally it is found[9] that superconducting F-doped LaOFeAs shows an intrinsic Josephson effect like bismuth cuprate[10] which is only possible if the spacer layers are not metallic and form tunnel barriers instead. The band

TABLE I. Structure parameters of bulk LaOFeAs. Note that GGA improves compared to LDA with respect to the lattice constants and the Fe-As distance d but not with respect to the As-Fe-As angles α and β on one side of and across the Fe layer, respectively.

	a (Å)	c (Å)	d (Å)	α β	z_{As}	z_{La}
Expt.	4.027	8.718	2.407	113.5 107.5	0.6513	0.1417
GGA	4.041	8.574	2.351	118.5 105.2	0.6403	0.1462
LDA	3.957	8.339	2.302	118.6 105.1	0.6410	0.1488

structure analysis of Fig. 1 indicates a conduction gap of several eV of the LaO layer. This is in contrast to $Ba(FeAs)_2$ where the Ba layers are obtained at least close to be metallic through Ba-5d orbitals.[4] Also seen in the figure by comparison of its left ($k_z=0$) with its right part ($k_z=\pi$) is the pronounced two-dimensional (2D) character of the conduction states.

We calculated also the bands for the experimental structure parameters. The deformation potentials with respect to change in the lattice constants and of the Wyckoff parameters for the Fe-3d bands crossing the Fermi level are typically 2 eV/Å. Both band structures deviate from each other less than 0.2 eV in the window ± 1 eV around Fermi level, which is irrelevant for our considerations. (The two nearly parallel dispersive bands along Γ-Z below Fermi level have Fe-3d_{z^2} character, which will appear even somewhat lower in energy if the experimental Wyckoff parameter is used instead of the GGA relaxed value (cf. Table I).) The unoccupied dispersionless La-4f bands are seen about 3 eV above Fermi level.

First we want to learn something on the cleavage behavior and the layer bonding. We adopt a model approach used in Ref. 11 in studying the cleavage of impure aluminum. To this goal, a periodic stacking of layers As/Fe/As/La/O/La/As/Fe/As/La/O/La is considered (in c direction doubled unit cell). The symmetry is lowered in this case to the orthorhombic space group Pmm2 so that all atom layers have free z Wyckoff parameters. (In the space group P4/nmm of the bulk crystal the z Wyckoff parameters of O and Fe layers are fixed by symmetry to the values 0 and 1/2, respectively.) Now, for a sequence of increasing c lattice constants the z Wyckoff parameters of all atom layers were relaxed. As will be seen from the results presented in the next section, the crystal is expected to cleave between As and La layers only. Hence, clean coherent As or La surfaces are expected after cleavage. In a real crystal, due to defects of course terraces will likely be obtained consisting of coherent As and La terminated areas, respectively.

Next, two types of symmetrically terminated periodically repeated slabs with the full space group P4/nmm are considered with atom layer stacking As/Fe/As/La/O/La/As/Fe/As/La/O/La/As/Fe/As and La/O/La/As/Fe/As/La/O/La/As/Fe/As/La/O/La (Fig. 2) with sufficiently large space between terminating surfaces so that subsequent slabs do not interact any more. For stacks of symmetric slabs this is easily obtained if there is sufficient space for the electronic states not to overlap across the spacing; due to symmetry there is no

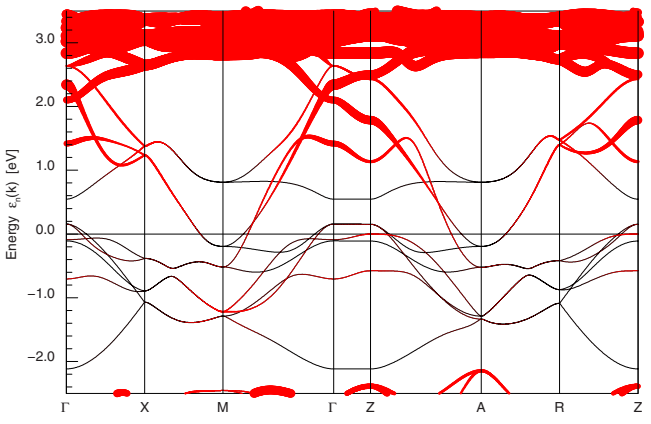

FIG. 1. (Color online) The Kohn-Sham GGA band structure of bulk LaOFeAs. The fat bands in red (shadow) weigh the O-2p and La-4f,5d,6s orbital contribution to the band state.

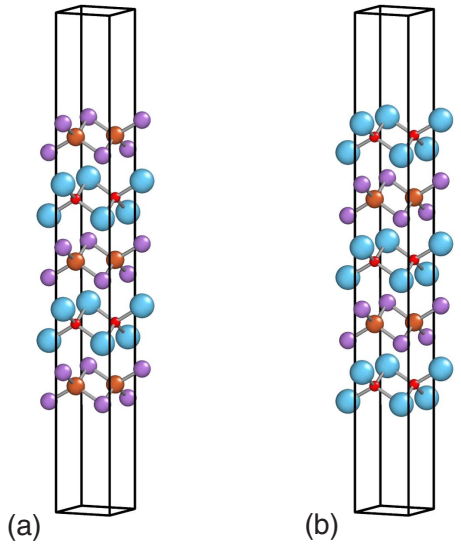

FIG. 2. (Color online) Slab geometry: unit cells of $(LaO)_4(FeAs)_6$ (a) and $(LaO)_6(FeAs)_4$ (b) slabs; blue (biggest spheres): La, red (smallest spheres): O, orange (medium, light): Fe, and violet (medium, dark): As.

electric field in the free space between the slabs. Since there are two atoms per Fe and O layer in the unit cell and one of the other atoms per layer, the unit cells of these stacks are $(LaO)_4(FeAs)_6$ and $(LaO)_6(FeAs)_4$, respectively.

To check that the results are representative for surfaces of bulk crystals both the spacing between the slabs and the slab thickness were varied. In addition to the above, $(LaO)_8(FeAs)_{10}$ and $(LaO)_{10}(FeAs)_8$ slabs are considered. Besides the results of structure relaxation, stability of layer charges is considered as a check for convergence of the considered slabs toward open bulk crystal surfaces. Given the total charge density of a crystal there is ambiguity to assign charges to the atom sites and different codes differ in doing so (if they make such an assignment at all). However, with such a charge partitioning procedure fixed, the stability of the assigned charges with respect to slab and spacer thickness can be taken as a criterion for size convergence. Here, the site charges recorded in the FPLO protocol file are used. As a result of these checks, while the slab $(LaO)_4(FeAs)_6$ turned out to be representative, the thicker slab $(LaO)_{10}(FeAs)_8$ had to be considered for the La terminated case.

Finally, for the geometrically relaxed slabs Kohn-Sham band structures were calculated and projected onto various basis orbitals of the "chemical basis" used in the FPLO code. This allows to distinguish bulk from surface bands and to estimate the spatial extension of the corresponding states. We mention here that FPLO works with a well designed small basis consisting at most of one "chemical" basis state (site orbital) and one polarization state per atomic orbital. The chemical relevance of the chemical part of the basis is emphasized by the fact that the polarization states are typically occupied by less than 0.01 electron in a converged calculation, although relaxed structures and total energies compete well in accuracy with any available full-potential density-functional code such as for instance FLAPW.

Geometry relaxation was done by direct calculation of the forces on atom sites and minimizing them with the corresponding tool of FPLO9.00. Convergence was accepted when all forces were smaller than 10^{-3} eV/Å. Only for the thickest slabs this was hard to achieve, and the relaxation was stopped when the atom positions did not change any more within 0.01 Å accuracy over several force steps (in an oscillating behavior) which keeps the band energies close to Fermi level within about 20 meV of accuracy.

III. RESULTS AND DISCUSSION

A. Cleavage behavior

Cleavage is ideally considered as expanding a bulk crystal in z direction until it disintegrates into parts. On the computer, a bulk crystal with a unit cell doubled in z direction and with the in-plane lattice constant fixed to its equilibrium bulk value $a=4.041$ Å, but with reduced space group to the orthorhombic group Pmm2 and with an increasing sequence of c lattice constants is treated. Pmm2 (still with $b=a$) is the highest symmetry of our situation which leaves all z Wyckoff parameters of all atom layers undetermined. For each value of the c lattice constant these Wyckoff parameters were relaxed in GGA.

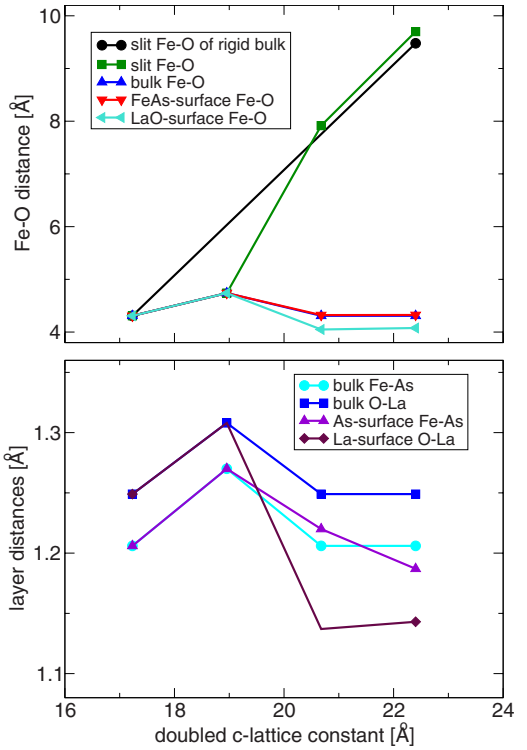

FIG. 3. (Color online) The atom layer distances as functions of the stretched c axis lattice constant. In the upper panel the Fe-O layer distances are shown, the two upper curves across the slit and the two lower curves between the surface and subsurface triple layer on both sides of the slit (FeAs and LaO terminated, respectively). On the lower panel the behavior of layer distances within the triple layers La/O/La and As/Fe/As, respectively, are shown, again for the bulk and for the surface triple layers. Observe the different scales of the ordinates. For more explanation see the text.

The crystal structure of LaOFeAs can be imagined as a stacking of layers of tetrahedra with their corners occupied with La and As sites, respectively, and which are centered by O and Fe ions (triple atom layers, Fig. 2). If the bulk structure of the crystal were rigid and the crystal would split between every fourth La-As layer pair, the slit width as measured between the Fe and O layers forming the centers of the adjacent tetrahedra layers would be that of the black straight line in the upper panel of Fig. 3. For z strain not exceeding about 10 percent (leftmost line segments in Fig. 3) the tetrahedra behave indeed as nearly rigid, but every La-As distance is homogeneously strained by one fourth of the black line. Observe that the ordinate scale is stretched by about a factor of 20 in the lower panel of Fig. 3 compared to the upper, so the changes in the La-O and Fe-As distances within the triple layers are really negligible compared to the change in the distance between the triple layers (smaller roughly by a factor of seven). Hence, for not to large strain the crystal behaves as a system of nearly rigid triple atom layers La/O/La and As/Fe/As which are elastically bonded together.

For a sufficiently small c strain of the crystal the original periodicity is preserved. However, as said the lattice essentially expands only between La and As layers while the La-O and As-Fe layer distances hardly change. There are four neighboring La-As layer pairs in the doubled unit cell. For

larger strain the original periodicity breaks up; some of the La-As layer distances snap back essentially to the bulk value while slits open at others. By the symmetry restriction of our approach (doubled periodicity in c direction), adopted to keep the computer time within reasonable limits, every fourth La-As spacing must open a slit. These results are shown on Fig. 3.

Somewhere between 10 and 20 percent z strain (we only calculated in 10 percent steps) this transition happens and the crystal cleaves. Because of our periodicity constraint it must simultaneously cleave between every fourth La-As layer pair. This behavior is seen in the middle straight line segments of Fig. 3. The layer distances where the crystal does not cleave snap back to approximately their equilibrium values and the distance at the cleavage slit approaches the black line. In truth this change is to be expected to happen abruptly somewhere between 10 and 20 percent strain, however, the actual value is not so interesting for our consideration. The layer distances do not exactly go back to their bulk values because the surface triple layers on both sides of the slit (one La/O/La and one As/Fe/As triple layer) relax a bit. As is seen the relaxation is much larger on the La side compared to the As side.

The clear message of these results is that LaOFeAs can only cleave between La and As while the La tetrahedra with O in the center and the As terahedra with Fe in the center are very stiff and stable. Also, in the elastic deformation regime the crystal is not only elastically extremely anisotropic, its unit cells also do not deform homogeneously under uniaxial stress as the bonds between triple layers of tetrahedra are almost one order of magnitude weaker than the bonds within the tetrahedra.

B. Surface relaxation

The approach of the previous section is correct as long as the width of the opening slit is still small enough so that both sides see each other. Because the produced slabs do not have a mirror plane, they produce a dipole charge density and hence electric fields across the slit. This does not describe the situation of a single surface of a crystal without its counterpart. As long as the sample is not charged this surface does not produce a far reaching electric field. This situation is better modeled by a symmetric slab of sufficient thickness to represent a half-crystal. Now, however, two different slabs with different possible surfaces have to be considered, which are As terminated and La terminated surfaces.

In order to model an As terminated surface, periodically repeated slabs $(LaO)_4(FeAs)_6$ and $(LaO)_8(FeAs)_{10}$ are considered with a separation of the slabs between about 13 and 30 Å. These structures have again the space group P4/nmm such as the bulk crystal, with a diagonal glide mirror plane in the middle. Therefore, these slabs do not produce gross dipole densities of the slab (of course, as any surface they have surface dipole densities, but here opposite to each other on both surfaces), and no electric fields are produced in the free space separating the slabs. They would only interact via wave function overlap across the slit. These slab structures were now relaxed using the forces on atom sites computed with the FPLO code. The obtained surface relaxation does practically not change, if the spacing between $(LaO)_4(FeAs)_6$ slabs is increased from 13 to 30 Å, and it stays within 0.02 Å, about twice the numerical accuracy of the calculation, between the $(LaO)_4(FeAs)_6$ and $(LaO)_8(FeAs)_{10}$ slabs.

As already in the cleavage process, the La terminated surface is more strongly relaxed than the As terminated surface. Moreover, it turns out that the $(LaO)_6(FeAs)_4$ slab is not thick enough in this case. The surface triple layer dopes more charge into the neighboring FeAs triple layer raising there the Fermi level against its bulk value. Besides the surface potential step, there are two more essential influences on the electronic structure of a slab structure relaxation and a chemical potential shift due to surface states. The latter is not operative on the surface of a bulk crystal where the chemical potential (Fermi level) is fixed to its bulk value. For this to be approximately true the $(LaO)_6(FeAs)_4$ slab turns out to be not thick enough. Therefore, we concentrate on a $(LaO)_{10}(FeAs)_8$ slab.

Table II shows the relaxed interlayer distances in comparison with their bulk values. For the As terminated slabs, essentially only the topmost triple layer relaxes by reducing the As-Fe layer distances by about 0.05 Å while all other distances inside triple layers stay at their bulk values within 0.01 Å accuracy. (Again, the bond between LaO and FeAs triple layers due to its weakness may relax somewhat more, 0.03 Å in one case.) For the La terminated surface the relaxation is much more dramatic, it amounts to an about 0.3 Å movement of the O position outwards from the center of the La tetrahedra. This continues into changes of about 0.03 Å of the Fe-As layer distances and even larger changes in the other layer distances inside the slabs.

As already mentioned in Sec. I, also the layer charges were compared with their bulk values in order to assess the quality of approaching the situation of a bulk crystal surface. As typical results, in Table III the GGA layer charges as obtained by FPLO are displayed for a bulk crystal, a cleaving crystal as described in subsection A, several As terminated slabs and for $(LaO)_{10}(FeAs)_8$. As one can see, the charge per unit cell of the central triple layer of the slabs deviate less than 0.01 electron charges from the bulk value, while for the unsymmetric slab of the cleavage situation the deviations are larger due to the additional electric field produced by the nonzero gross dipole density.

C. As terminated surface

As can be inferred from Tables II and III, the central Fe-As triple layer of $(LaO)_4(FeAs)_6$ is already close to a bulklike state. Also the Fermi level relative to the bands derived from this central layer is bulklike. Therefore, the band structure of this slab shown in Fig. 4 may be considered as representative for a bulk crystal with an As terminated (001) surface. Observe that the slab bands do not have k_z dispersion due to the slab confinement of the Kohn-Sham states. As is seen in Fig. 1, the k_z dispersion of the bulk bands crossing Fermi level is also negligible. Therefore, in the following only the in-plane dispersion of the bands is discussed and presented in the figures.

TABLE II. GGA relaxed interlayer distances in Å for the bulk crystal and for various slabs. In view of the mirror symmetry only half of each slab is presented: its center is at the lower end and the surface is indicated by a dashed line.

	Bulk	$(LaO)_4(FeAs)_6$	$(LaO)_8(FeAs)_{10}$	$(LaO)_6(FeAs)_4$	$(LaO)_{10}(FeAs)_8$
…	…				
As/Fe	1.203	1.146	1.150		
Fe/As	1.203	1.161	1.168		
As/La	1.830	1.815	1.830		
La/O	1.254	1.249	1.255	0.940	0.948
O/La	1.254	1.244	1.248	1.536	1.529
La/As	1.830	1.799	1.832	1.420	1.436
As/Fe	1.203	1.193	1.202	1.198	1.206
Fe/As	1.203	…	1.201	1.179	1.168
As/La	1.830		1.831	1.803	1.871
La/O	1.254		1.253	1.243	1.208
O/La	1.254		1.254	…	1.263
La/As	1.830		1.831		1.729
As/Fe	1.203		1.202		1.172
Fe/As	1.203		…		1.179
As/La	1.830				1.696
La/O	1.254				1.222
…	…				…

TABLE III. FPLO GGA cross layer charges in (positive) elementary charges per atom of bulk and cleaved (second column) LaOFeAs and of various slabs of it. The number after the colon in the headings gives the slit thickness in multiples of bulk c lattice constants. Only the upper half of the last symmetric slab is presented. In parentheses the charges of the covalently bound triple layers are given.

Layer	Bulk	$(LaO)_4(FeAs)_4$:2.6c	$(LaO)_4(FeAs)_6$:4c	$(LaO)_4(FeAs)_6$:6c	$(LaO)_8(FeAs)_{10}$:6c	$(LaO)_{10}(FeAs)_8$:6c
	…					
As	−0.738	−0.358	−0.179	−0.179	−0.177	
Fe_2	+0.287 (−1.189)	+0.392 (−0.731)	+0.299 (−0.611)	+0.297 (−0.608)	+0.307 (−0.609)	
As	−0.738	−0.765	−0.731	−0.726	−0.735	
La	+1.954	+1.959	+1.955	+1.955	+1.955	+1.467
O_2	−2.719 (+1.189)	−2.701 (+1.215)	−2.706 (+1.199)	−2.707 (+1.198)	−2.706 (+1.199)	−2.436 (+0.786)
La	+1.954	+1.947	+1.950	+1.950	+1.950	+1.755
As	−0.738	−0.726	−0.722	−0.719	−0.734	−0.840
Fe_2	+0.287 (−1.189)	+0.272 (−1.229)	+0.267 (−1.177)	+0.258 (−1.180)	+0.291 (−1.182)	+0.233 (−1.303)
As	−0.738	−0.777	−0.722	−0.719	−0.739	−0.696
La	+1.954	+1.849	+1.950	+1.950	+1.954	+1.954
O_2	−2.719 (+1.189)	−2.445 (+0.767)	−2.706 (+1.199)	−2.707 (+1.198)	−2.719 (+1.187)	−2.727 (+1.172)
La	+1.954	+1.363	+1.955	+1.955	+1.954	+1.945
As	−0.738		−0.731	−0.726	−0.739	−0.738
Fe_2	+0.287 (−1.189)		+0.299 (−0.611)	+0.297 (−0.608)	+0.288 (−1.190)	+0.192 (−1.252)
As	−0.738		−0.179	−0.179	−0.739	−0.707
La	+1.954				…	+1.956
O_2	−2.719 (+1.189)					−2.718 (+1.194)
La	+1.954					+1.956
	…					…

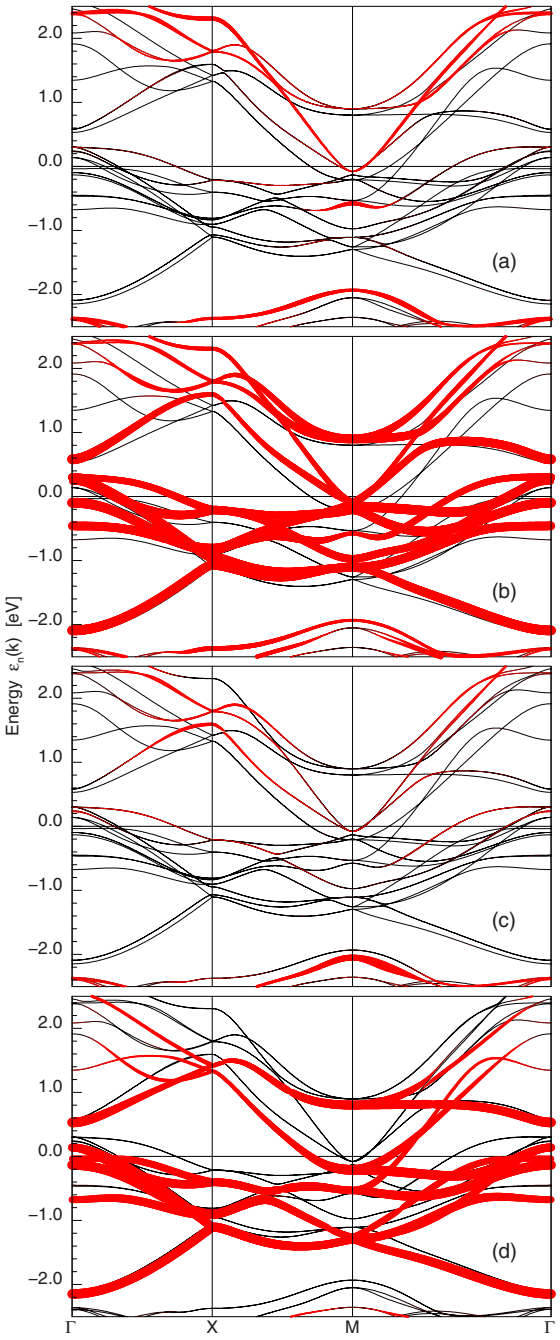

FIG. 4. (Color online) Band structure of the $(LaO)_4(FeAs)_6$ slab. The thickness of the red (shadow) lines represents in turn the orbital weight of (a) surface As 4*p*, (b) subsurface Fe 3*d*, (c) subsurface As 4*p*, and (d) central (bulk) Fe 3*d*.

By the thickness of colored lines, the orbital character of the bands is indicated in Fig. 4 from top to bottom for basis orbitals in which the Kohn-Sham band wave functions are expanded; of surface As 4*p* orbitals, Fe 3*d* orbitals of the Fe layer below the surface As layer, As 4*p* orbitals of the next layer below this Fe layer, and finally of the Fe 3*d* orbitals in the center of the slab which corresponds to the first Fe layer below the surface triple layer of a bulk crystal. The latter Fe atoms are about 10 Å below the position of the surface As atoms.

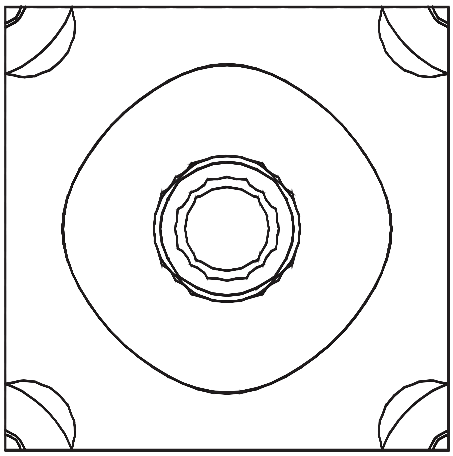

FIG. 5. The 2D FSs of the slab $(LaO)_4(FeAs)_6$. The zone center is Γ and the corner point is *M*. From Γ outward in turn the FSs are two times bulk, three times surface; from *M* outward: two tiny surface FSs, two bulk FSs. (The small wiggles are due to the resolution of the used $\boldsymbol{k}$ mesh.)

The Kohn-Sham band wave functions in the vicinity of Fermi level are formed by the above accounted chemical basis orbitals to about 99% so that the thick colored lines of Fig. 4 (and also of Fig. 6 below) completely represent the extension of the corresponding Kohn-Sham wave functions. Polarization states and other basis states besides the explicitly discussed, of the full basis used in the calculations do not contribute to these Kohn-Sham wave functions.

Both the surface Fe 3*d* bands and the bulk Fe 3*d* bands cross the Fermi level, however, they form quite different Fermi surfaces (FS) as shown in Fig. 5. Around Γ there are two hole cylinders of bulk bands and around *M* there are two electron cylinders, all much like in a bulk crystal calculation without surface. Note that in the slab $(LaO)_4(FeAs)_6$ on which Fig. 5 is based the surfaces FSs are (almost) twofold degenerate due to the two surface FeAs triple layers on both sides of the slab (which do almost not interact due to the *z* confinement of all conduction states within As/Fe/As triple layers). Hence, each of the surface FSs is doubly degenerate which is, however, not resolved in the figure.

There is next to no contribution of orbitals in the subsurface LaO triple layer as well as in any LaO triple layer to these bands (cf. Fig. 1). There the Kohn-Sham wave function amplitude is already reduced by about an order of magnitude.

As seen in panel (b) of Fig. 4, there are three surface bands forming FS hole cylinders around Γ. Two of them have radii only slightly larger than the bulk FSs but one has a radius more than twice as large. It results from a band of Fe $3d_{z^2}$ orbital character which is completely occupied in the bulk. Since all conduction bands of these materials are Fe-As antibonding,[4] it is shifted up by the surface compression of the As tetrahedra in *z* direction strengthening the FeAs covalency of the $3d_{z^2}$ orbital with the As 4*p* orbitals around Γ ($\boldsymbol{k}=0$).

There are again two electron cylinders around *M*, but they are tiny having radii about three times smaller than the corresponding bulk FSs. The surface states are essentially only

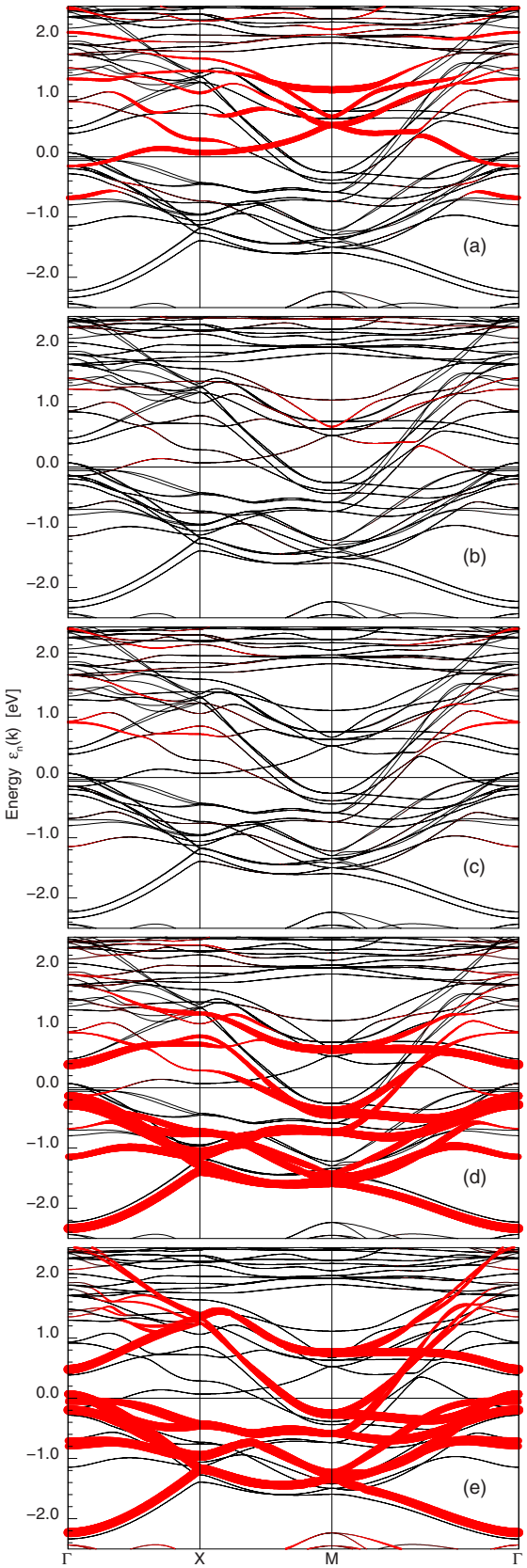

FIG. 6. (Color online) Band structure of the $(LaO)_{10}(FeAs)_8$ slab. The thickness of the red (shadow) lines represents in turn the orbital weight of (a) surface La $5d+6s$, (b) subsurface O $2p$, (c) subsurface La $5d+6s$, (d) next to surface Fe $3d$, and (e) inner (bulk) Fe $3d$.

formed by Fe $3d$ orbitals of the surface triple layer. They have very small amplitudes everywhere else.

D. La terminated surface

Table II says that the surface relaxation of an LaO surface triple layer is dramatic. While the geometry of the La tetrahedra changes little, the O sites move outward by about 0.3 Å. The charge per unit cell of the O layer changes by 0.3 electron charges compared to the bulk while in the case of a FeAs surface triple layer the corresponding change in the Fe charge was only within 0.02 electron charges. The subsurface La layer charge still changes by 0.2 electron charges which induces even some change in the next FeAs triple layer and only beneath that a near bulk situation is found. In contrast, only the charge of the topmost As atom layer differs noticeably from the bulk value in the case of the As terminated surface.

Correspondingly dramatic are the changes in the surface electronic structure presented on Fig. 6. In contrast to the inner LaO triple layers the topmost La layer is conducting. The electron attractive potential of the O ions moving closer to the topmost La sites brings the outermost La $6s$ bands down in energy by about 2 eV compared to its bulk position so that it crosses Fermi level forming a large electron cylinder FS around Γ, see. Fig. 7. This is another case of the strong polarizability of oxygen in transition metal oxide compounds related to the resonant instability of the O^{2-} ion.

As Fig. 7 is based on the results for the slab $(LaO)_{10}(FeAs)_8$, all FSs shown are again twofold degenerate, and a noticeable splitting is only seen for the second FS around M due to a small interaction of the subsurface FeAs triple layers via the next deeper FeAs layers. Note also that the 'bulk' FSs of the figure are slightly shrunk around Γ and expanded around M compared to true bulk FSs. This is because the slab $(LaO)_{10}(FeAs)_8$ is still not thick enough for the Fermi level to converge to its bulk value. There would,

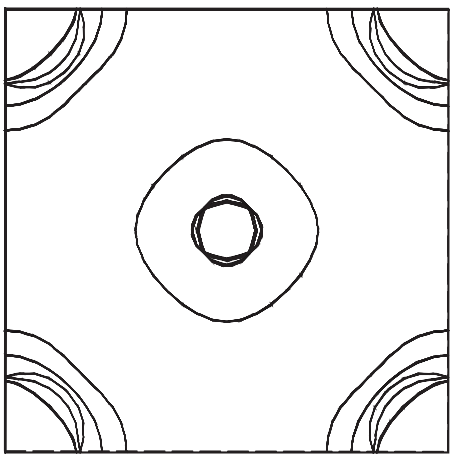

FIG. 7. The 2D FSs of the slab $(LaO)_{10}(FeAs)_8$. Compare Fig. 5. The FSs from Γ outward are two times bulk Fe $3d$, the outer one surface La $6s$; from M outward two times bulk Fe $3d$, the second one split in the slab, see text for explanation, two outer subsurface Fe $3d$ FSs.

however, be no change in the character of the results any more for even thicker slabs.

The wave function of the La surface band is essentially decayed already at the neighboring O layer and there is a barrier for states at Fermi level down to the next Fe layer (about 4 Å wide). This Fe layer still has strongly deformed bands compared to the bulk with no FS around Γ and two quite large hole cylinders around *M*. Only at the next deeper Fe layer (about 14 Å beneath the crystal surface) the wave function of the bulk bands starts off.

Hence, the subsurface FeAs triple layer bands of an La terminated surface deviate just in the opposite direction from the bulk compared to the surface FeAs triple layer bands of an As terminated surface they shrink to zero at Γ and expand substantially around *M*. In addition a conducting surface La 6*s* band forms a large electron cylinder around Γ.

IV. SUMMARY AND CONCLUSIONS

Due to the layered structure of the recently discovered iron based superconductor materials, their electronic structure is to various degrees quasi-2D, most pronounced in LaOFeAs, the material considered in this paper. As expected this situation gives rise to a well developed and perpendicular to the crystal surface well localized surface band structure which appears to be dramatically different from that in the bulk.

Closely interrelated with this deviating surface electronic structure are quite strong surface relaxations of the crystal structure, in the considered material most dramatic for the La terminated surface. Numerical structure relaxations reveal that LaOFeAs has quite stiff LaO and FeAs triple layers as structural subunits which are bound together in a much weaker way. As a result, tensile stress in *z* direction practically only expands the distance between these subunits and hardly changes these substructure bond lengths themselves. This is why in a cleavage process very coherent As and La terminated surfaces are expected only.

Since the structural subunits are mutually charged and those charges are separated in the cleavage process, the strong surface relaxations are even enhanced and the surface triple layers now also internally relax mainly due to their change in charging. While the As tetrahedra shrink in *z* direction keeping the Fe ions close to their centers, the La tetrahedra remain nearly unchanged, but the O ions move out of their centers by about 0.3 Å. This is related to a strong change in the ionization state of the O ion, while the ionization state of the Fe ions is hardly changed at the surface. Only the topmost As ions change their ionization state strongly as expected due to the missing doping counterpart, and, of course, also such as the topmost La ions of the La terminated surface.

Both the As and La terminated surfaces develop a 2D surface band structure of in *z* direction well confined band states while the bulk band states are dying off between 10 and 8 Å below the surface As sites of an As terminated surface and even about 4 Å deeper in the case of an La terminated surface. Both surface band structures develop FSs. For the As terminated surface and compared to bulk these FSs are expanded around Γ and shrunk nearly to zero at *M*. Not really a surprise, an additional FS appears of a band of predominantly Fe $3d_{z^2}$ orbital character (which is completely occupied in the bulk). It is another hole FS with a large radius around Γ and, due to its orbital character its wave functions are closest to the surface. For the La terminated surface, on the opposite, the FSs around Γ disappear completely for the surface bands while those around *M* are expanded. However, as a real surprise, an electron FS around Γ appears with a medium radius, which has La 6*s* orbital character. Toward zone boundary the orbital character of this band continuously changes into mainly La $5d_{xz}$ and $5d_{yz}$. Compared to the bulk the corresponding states are lowered in energy by about 2 eV by forming a most strong covalent bond with the O neighbor. It is this energy gain which moves the O ion out of the center of the La tetrahedron.

These surface band structures must be expected strongly to influence any surface sensitive experimental result. In particular, it seems to us that ARPES results for NdOFeAs (Ref. 12) (doped with F) as well as of LaOFeAs (Ref. 13) show tendencies of As terminated surfaces. In Ref. 12, Fig. 1 a large Fermi radius around Γ is seen and in Ref. 13, Fig. 2 (panel d) the Fermi surface around Γ of the surface state is clearly visible.

ACKNOWLEDGMENTS

We gratefully acknowledge assistance by U. Nitzsche with the use of computer facilities. We thank A. Koitzsch and J. van den Brink for helpful discussions.

*k.koepernik@ifw-dresden.de; http://www.ifw-dresden.de/~/magru

[1] Y. Kamihara, T. Watanabe, M. Hirano, and H. Hosono, J. Am. Chem. Soc. **130**, 3296 (2008).
[2] V. I. Anisimov, D. M. Korotin, M. A. Korotin, A. V. Kozhevnikov, J. Kuneš, A. O. Shorikov, S. L. Skornyakov, and S. V. Streltsov, J. Phys.: Condens. Matter **21**, 075602 (2009).
[3] D. J. Singh, Physica C **469**, 418 (2009).
[4] H. Eschrig and K. Koepernik, Phys. Rev. B **80**, 104503 (2009).
[5] www.fplo.de; see also K. Koepernik and H. Eschrig, Phys. Rev. B **59**, 1743 (1999).
[6] J. P. Perdew, K. Burke, and M. Ernzerhof, Phys. Rev. Lett. **77**, 3865 (1996).
[7] J. P. Perdew and Y. Wang, Phys. Rev. B **45**, 13244 (1992).
[8] T. Nomura, S. W. Kim, Y. Kamihara, M. Hirano, P. V. Sushko, K. Kato, M. Takata, A. L. Shluger, and H. Hosono, Supercond. Sci. Technol. **21**, 125028 (2008).
[9] Paul Müller (private communication).
[10] R. Kleiner, F. Steinmeyer, G. Kunkel, and P. Müller, Phys. Rev. Lett. **68**, 2394 (1992); L. Ozyuzer, Y. Simsek, H. Koseoglu, F. Turkoglu, C. Kurter, U. Welp, A. E. Koshelev, K. E. Gray, W. K. Kwok, T. Yamamoto, K. Kadowaki, Y. Koval, H. B. Wang, and P. Müller, Supercond. Sci. Technol. **22**, 114009 (2009).
[11] L. Goodwin, R. J. Needs, and V. Heine, J. Phys.: Condens. Matter **2**, 351 (1990).

[12] Ch. Liu, T. Kondo, A. D. Palczewski, G. D. Samolyuk, Y. Lee, M. E. Tillman, N. Ni, E. D. Mun, R. Gordon, A. F. Santander-Syro, S. L. Bud'ko, J. L. McChesney, E. Rotenberg, A. V. Fedorov, T. Valla, O. Copie, M. A. Tanatar, C. Martin, B. N. Harmon, P. C. Canfield, R. Prozorov, J. Schmalian, and A. Kaminski, Physica C **469**, 491 (2009).

[13] D. H. Lu, M. Yi, S.-K. Mo, J. G. Analytis, J.-H. Chu, A. S. Erickson, D. J. Singh, Z. Hussain, T. H. Geballe, I. R. Fisher, and Z.-X. Shen, Physica C **469**, 452 (2009).